JOURNAL OF PROPULSION AND POWER
Vol. 11, No. 1, January–February 1995

NOx Model for Lean Combustion Concept

N. K. Rizk* and H. C. Mongia†
General Motors Corporation, Indianapolis, Indiana 46206

In an effort to reduce the emissions produced by gas turbine combustors to meet the expected trends of more stringent regulations, a model to calculate NOx produced by lean combustion concepts is proposed. The model simulates the combustor by a number of reactors representing the main combustion as well as pilot zones. A detailed reaction rate scheme was used to provide a fundamental basis for the derivation of reaction temperature and NOx formation expressions. The model validation involved the utilization of the data obtained for a combustor that comprised a prechamber in which fuel was vaporized and mixed with air, and a variable geometry feature to control air split between various zones. In addition to the satisfactory agreement with the measurements obtained under a wide range of operations, the model provided insight into the roles of the primary zone and pilot in forming NOx. The present investigation also shows that multidimensional calculations can provide important assistance for emissions model development. Methods of NOx reduction may be implemented in light of such information.

Nomenclature

$F1$	=	flow model parameter
P_3	=	inlet pressure, kPa
T	=	reaction temperature, K
T_{eq}	=	equilibrium temperature, K
T_3	=	inlet temperature, K
VG	=	variable geometry position, m
Z	=	location of plane in modeled sector, deg
$\Delta P_3/P_3$	=	combustor pressure drop
τ	=	residence time, ms
τ_{eq}	=	equilibrium residence time, ms
τ_p	=	residence time in pilot, ms
τ_r	=	residence time in recirculation zone, ms
ϕ	=	equivalence ratio

I. Introduction

A GAS turbine combustor is required to be designed and developed to achieve high combustion efficiency over a wide operating envelope while maintaining low NOx emissions and smoke, low flame stability limits, and good starting characteristics. Moreover, the combustion system should demonstrate low pressure loss and pattern factor with sufficient cooling air assigned to maintain low wall temperature levels for enhanced structural durability. To meet these mutually conflicting design requirements, it is essential to gain better understanding of the complex flowfield around and within the combustor liner. The flow includes swirl, recirculation, fuel injection, atomization, fuel evaporation, mixing, turbulent combustion, and convective and radiative heat transfer processes.

Because of the expected trends of more stringent emissions regulations, coupled with the fact that the combustor will be required to operate at higher temperatures and pressures, more advanced combustion systems are sought for future applications. For instance, current diffusion flame combustors operating on typical aviation fuels emit significant levels of NOx due to the high temperature created in regions having sufficient concentration of fuel, atmospheric nitrogen, and oxygen.

Because the rate of NOx formation significantly increases with local flame temperatures, the effort has been made to develop combustor concepts that operate at lower reaction zone temperatures. It has been shown that a fuel-rich combustion zone can be effective in reducing NOx.[1,2] The success of such a concept relies on the rapid quench required for the transportation of the rich mixture to the lean zone of the combustor where the balance of the fuel is oxidized. On the other hand, if a primary zone equivalence ratio of conventional combustors is reduced, the nonuniformities in fuel distribution and spray burning can still produce high local temperatures that are favorable for excessive NOx formation. To separate the mixing and reaction step entirely, a method was proposed that consists of prevaporizing and premixing the fuel with air prior to combustion.[3–5] Satisfactory performance of such a lean concept over the whole engine cycle is usually maintained by controlling the stoichiometry in the combustion zone by means of variable geometry devices.[6,7]

To optimize the combustor design, both empirical and analytical methods are required to provide insight into the combustion and mixing processes within the combustor flowfield. Empirical approaches based on a wide data base have been successfully used in various phases of combustor development. These methods require the accurate estimate of important parameters such as length or volume occupied in combustion, recirculation zone characteristics, and the fraction of air used in primary zone combustion.[8,9] Empirical correlations that provide estimates of NOx formation in various combustion zones of low-NOx combustor applications are given in Refs. 2 and 10.

On the other hand, in order to achieve significant advances in technology, a detailed representation of the combustor flow made available through an analytical method should be utilized in the effort.[11] Because of the incomplete understanding of various combustion processes and numerical diffusion, the prediction capabilities of the multidimensional models of performance and emissions are rather limited. In recent years, the effort has been made to combine three-dimensional calculations with proven empirical expressions to yield quantities of interest to the combustor designer.[12,13] The approach has been successfully applied to diffusion flame combustors as well as rich-lean and premixed/prevaporized concepts.[2,10]

To enhance the simulation of the reaction mechanism used in the emission calculations, a finite-rate chemistry scheme

Presented as Paper 92-3341 at the AIAA/SAE/ASME/ASEE 28th Joint Propulsion Conference and Exhibit, Nashville, TN, July 6–8, 1992; received April 12, 1993; revision received May 4, 1994; accepted for publication May 9, 1994.

*Staff Research Scientist, Allison Gas Turbine Division. Associate Fellow AIAA.

†Chief, Combustor R&D, Allison Gas Turbine Division. Member AIAA.

was used to provide the trends of the pollutant formation and consumption in various combustion zones. Based on the results of these calculations, expressions were developed to account for the effects of system pressure, residence time, reaction temperature, and equivalence ratio on emission concentrations. This approach has demonstrated promising results when applied to rich-lean combustor,[14] and to a conventional diffusion flame combustor.[15]

In the present investigation, the modeling of the pollutant formation using detailed reaction mechanism to provide the elements of the model has been extended to address lean prevaporized/premixed combustion concepts. The model simulates the reaction in the combustor by a number of reactors that represent different zones. The validation of the approach utilized the experimental data of the AGT 100 combustor that employed a variable geometry mechanism to control air admission into various combustor zones. In the next section, a review of relevant NOx models is given, followed by the details of the proposed calculation approach. The results of the model validation and a summary of the main conclusions are given in later sections of this article.

II. NOx Modeling

The exhaust concentration of the pollutants are governed by the mean residence time in the combustion zone, the reaction rates, and mixing rates. Oxides of nitrogen NOx are produced in the central hot region of the combustor by the oxidation of the atmospheric nitrogen, and most of the NOx emitted in the exhaust is nitric oxide NO. If fuels contain organically bound nitrogen, then some of this nitrogen will eventually form fuel NO. Temperature has a less significant effect on the formation of fuel NO. Prompt NO is produced by the oxidation of nitrogen involving hydrocarbon species in the flame zone. In most cases, the prompt NO is only a small fraction of the NO formed in the postflame zone.

Lefebvre[8] utilized a large amount of data obtained for a number of production engines to reach a quantitative relationship for NOx. In his correlation, the NOx present in the exhaust is assumed to vary with the system pressure raised to a power of 0.25, residence time in the primary zone, and an exponential term that includes the stoichiometric temperature. Rizk and Mongia[10] followed a similar approach to derive an expression for NOx emission from lean prevaporized/premixed combustors. The expression comprises two terms representing NOx formation in a primary zone, in addition to the formation in the combustor pilot zone. Appropriate reaction temperature and residence time in each zone are used in the equation. An acceptable operating envelope for low NOx formation was defined using the developed expression.

Buchheim[16] proposed a mechanism of NOx formation that considers the NOx concentration at the combustor exit to be governed by the residence time at stoichiometric conditions. Based on the Zeldovich mechanism described in Ref. 17, an expression relating NOx to a fraction of fuel reacting at stoichiometric fuel/air ratio was developed. The reaction rate in this expression is based on stoichiometric temperature, and the NOx is assumed to vary with the square root of pressure. He showed that, in contrast to conventional gas turbine combustors, a lean premixed combustion system is capable of simultaneously meeting low NOx and low CO goals.

Several analytical models have been proposed in the literature to correlate pollutant formation within the combustor. These models consist of a number of chemical reactors that simulate various regions of the combustor. Hammond and Mellor[18] described a model based on the combination of a number of perfectly stirred reactors that utilized a global finite rate mechanism. Volumes of reactors and flow splits were selected to yield best fits with the internal measurements of NO and CO. They attributed the poor predictions of the variation of the emissions with the combustor loading to neglecting the heterogeneous effects.

Fletcher and Heywood[19] modeled the combustor primary zone as partially stirred reactor burning gaseous fuel over a distribution about the primary zone equivalence ratio, a lateral mixing reactor, and a plug flow reactor. Two model-fitting parameters were used in the model that gave satisfactory correlation with NOx data, except at low power mode.

A flow model that simulated a combustor operating on the rich/lean combustion concept was presented by Rizk and Mongia.[14] It consists of a rich zone made up of two parallel stirred reactors feeding into a plug flow reactor. Mixer air is admitted consequentially into the system to simulate quench and lean zones. A chemical kinetic mechanism that involves a large number of standard reactions was used to evaluate the relative contribution of various combustion zones to the total NOx formation. A similar approach was followed to develop an emission model for conventional diffusion flame combustors.[15] The success of such an approach to satisfactorily correlate the experimental data of both combustion concepts indicates the potential of extending the model to simulate lean premixed/prevaporized NOx formation. In the next section, the details of the proposed NOx model for lean combustors are described.

III. Lean Combustor NOx Model

To develop a NOx model that utilizes a chemical kinetic scheme for the lean combustion concept, the combustor was simulated by the flow model shown in Fig. 1. The flow model consists of a primary zone made up of two parallel stirred reactors: 1) a recirculation zone reactor and 2) a near-wall reactor. In prevaporization/premixed combustion systems fuel vapor and air are mixed prior to entering these two reactors. Extra air is allowed to enter the near-wall zone if the combustor includes dome air holes. A reactor to simulate the combustor pilot, which is usually incorporated in the combustor for lightoff and as a flame sustainer source, is also accounted for in the model. Fuel is admitted into the reactor in the liquid phase condition. The outcome of these reactors is fed into a main plug reactor where the combustion gases continue to react. Dilution air is mixed with the combustion gases leaving the main reactor.

A. Reaction Rate Mechanism

The reaction mechanism, used to provide the basis for the proposed NOx model, combines a global reaction for the breakdown of the hydrocarbon fuel to carbon monoxide and hydrogen with finite rate equations for the combustion of CO and H_2 and the formation of nitrogen oxides. The global reaction is given by the following equation:

$$C_xH_y + (x/2)O_2 \rightarrow xCO + (y/2)H_2 \quad (1)$$

The present reaction scheme involves the calculation of NO via the extended Zeldovich mechanism.[17] Examples of the key reactions are as follows:

$$O + N_2 \rightarrow NO + N \quad (2)$$

$$N + O_2 \rightarrow NO + O \quad (3)$$

$$NO + OH \rightarrow NO + H \quad (4)$$

To evaluate the relative contribution of each combustion zone to the total NOx formation, a wide range of operating parameters, that are typical of those of the lean combustors, was covered in a parametric study using the reaction scheme. The critical issues addressed in this study were the effects of combustor inlet temperature and pressure, equivalence ratio, and residence time in each reactor on the reaction temperature and NOx formation in each individual reactor. The investigation covered ranges of inlet temperature of 977–1200 K, pressure of 149–1448 kPa, equivalence ratio of 0.05–0.7, and residence time up to 16 ms.

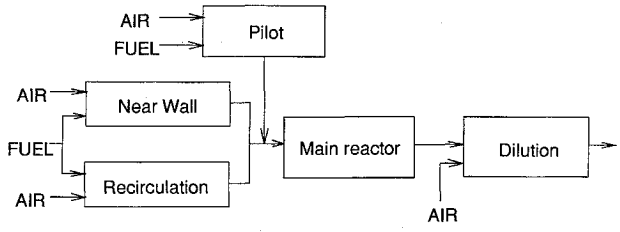

Fig. 1 Proposed combustor flow model.

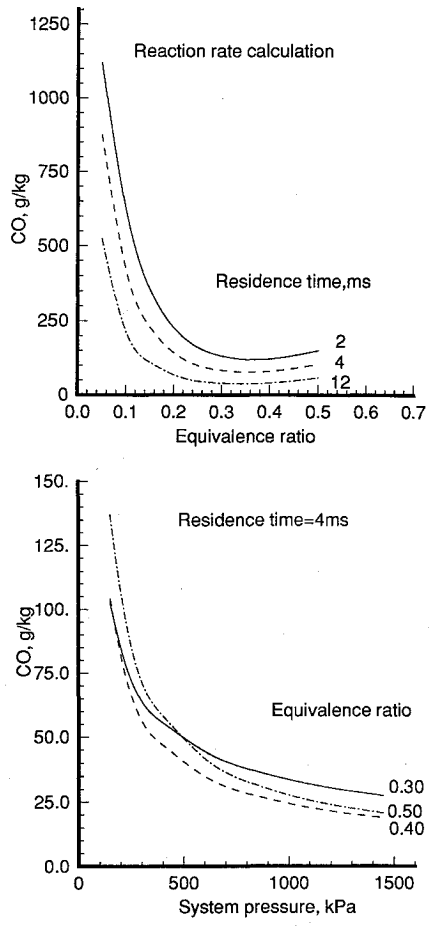

Fig. 2 Reaction rate calculation of CO.

In order to derive expressions that could be used to evaluate the NOx formation in each combustor zone, it is essential to obtain an accurate estimate of the reaction temperature that may be significantly lower than the readily available equilibrium temperature. The presence of CO in the products of fuel lean reaction is an indication of combustion inefficiency. To illustrate the effects of various parameters on the completion of the combustion, the values of the CO calculated by the kinetic scheme are plotted in Fig. 2. Any increase in residence time, equivalence ratio, or system pressure will reduce the CO concentration, bringing it closer to the equilibrium value of the CO encountered under fuel lean conditions.

B. Reaction Temperature Calculations

A number of expressions have been derived to calculate the reaction temperature in the various reactors shown in Fig. 1 in terms of T_{eq} and τ. For the primary zone reactors that are supplied with mixture of fuel vapor and air, the reaction temperature is calculated by

$$T = T_{eq} \exp[-n(1/\tau^{0.7} - 1/\tau_{eq}^{0.7})] \quad (5)$$

The residence time needed to reach equilibrium τ_{eq} varies with equivalence ratio, inlet temperature, and pressure as given by the following correlations:

$$\tau_{eq} = \tau_{t3} \cdot \tau_p \cdot [28.24\phi^{2.1} \exp(0.34\phi^{-1.4})] \quad (6)$$

where

$$\tau_{t3} = (T_3/1089)^A \exp[B(T_3^{-4.9} - 1.31E - 15)] \quad (7)$$

$$\tau_p = \exp[C(P_3^{-0.8} - 0.014)] \quad (8)$$

The parameters A, B, and C are calculated by

$$A = -1.25 + 36.5(\phi - 0.2) \quad (9)$$

$$B = 10E15[0.36 - 4.83(\phi - 0.2)] \quad (10)$$

$$C = 307.47 \exp(-0.0047/\phi^{3.5}) \quad (11)$$

Similarly, exponent n in Eq. (5) is given by

$$n = n_\phi \cdot (T_3/1089)^D \cdot (P_3/207)^E \quad (12)$$

where

$$n_\phi = 0.034 + 0.138\phi - 1.191\phi^2 + 3.25\phi^3 - 2.64\phi^4 \quad (13)$$

The exponents D and E are defined as follows:

$$D = -4.77 + 13.73\phi \quad (14)$$

$$E = -1.216\phi^{0.49} \quad (15)$$

Figure 3 shows examples of the reaction temperature variation with residence time and equivalence ratio as calculated by the reaction rate scheme, as well as by the correlation given by Eq. (5). The equilibrium temperatures are also plotted in the figure. Also illustrated in the second part of this figure is the effect of the system pressure on the reaction temperature. The results shown in this figure indicate that the

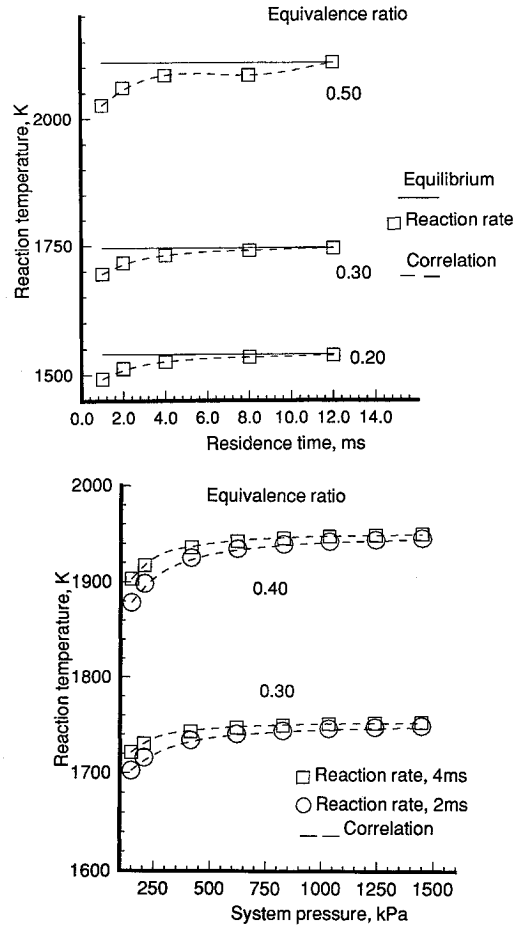

Fig. 3 Variation of reaction temperature with operating parameters.

correlation provides accurate estimates of the reaction temperature under various operating conditions.

The effects of liquid fuel evaporation on the reaction temperature of the pilot zone T_p are accounted for by using the following equation:

$$T_p = T/[0.968T_3^{0.0056}\phi_p^{0.0026} \exp(0.003\tau_p^{-2})] \quad (16)$$

where T is the reaction temperature of fuel vapor/air mixture given by Eq. (5), and ϕ_p is the equivalence ratio in pilot zone.

C. Proposed NOx Model

The results provided by the chemical reaction scheme for a wide range of operation were used as a basis for the development of the NOx model. A number of expressions have been formulated to simulate the NOx formation mechanism in various reactors. In the primary zone reactors, the NOx formation is expressed by the following equation:

$$\text{NOx (g/kg)} = 0.7E - 16N_\phi \cdot N_p \cdot T^{1.3} \exp(0.943T^{0.45})(\tau/2)^{an} \quad (17)$$

The dependency of NOx on equivalence ratio N_ϕ is described by the following expressions:

$$N_\phi = 0.426 + 25.85\phi - 178.1\phi^2 + 473.1\phi^3 - 558.5\phi^4 + 245.6\phi^5 \quad (18)$$

For an equivalence ratio less than 0.2, the dependency of NOx on equivalence ratio is more accurately described by

$$N_\phi = 1.36E - 15T_3^{5.0} \exp(-0.073/\phi) \quad (19)$$

The pressure term N_p in Eq. (17) is calculated from the following expression:

$$N_p = (P_3/207)^b \exp[-c(P_3^{-0.3} - 0.2)] \quad (20)$$

The parameters b and c vary with the equivalence ratio as given by the following equations:

$$b = 2.33\phi^{2.15} - 0.475 \quad (21)$$

$$c = 150.2 - 170.7\phi^{0.2} \quad (22)$$

The exponent an for τ is given by

$$an = an_\phi(T_3/1089)^{am}(P_3/207)^{b1} \cdot \exp[c1(P_3^{-0.3} - 0.2)]/f \quad (23)$$

where

$$an_\phi = 0.14\phi^{-0.9} \exp(3.33\phi^{2.4}) \quad (24)$$

For ϕ below 0.2

$$an_\phi = 0.52 + 11.65\phi - 102.5\phi^2 + 235.9\phi^3 \quad (25)$$

The parameters $b1$, $c1$, and am are given by

$$b1 = 11.58\phi^{1.8} - 2.78 \quad (26)$$

$$c1 = 187.3\phi^{0.68} - 102.3 \quad (27)$$

$$am = 4.59\phi - 2.43 \quad (28)$$

The factor f is calculated from

$$f = 1.3 - 4.2\phi + 33.7\phi^2 - 88.5\phi^3 + 72.6\phi^4 \quad (29)$$

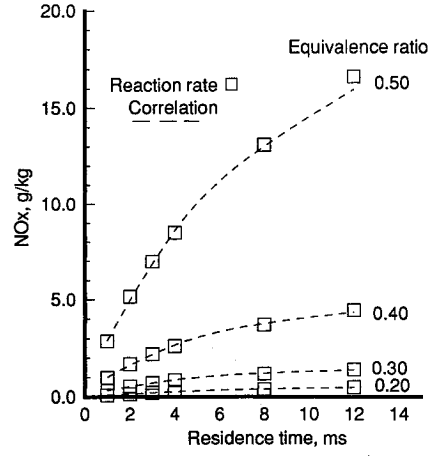

Fig. 4 NOx prediction by developed correlation.

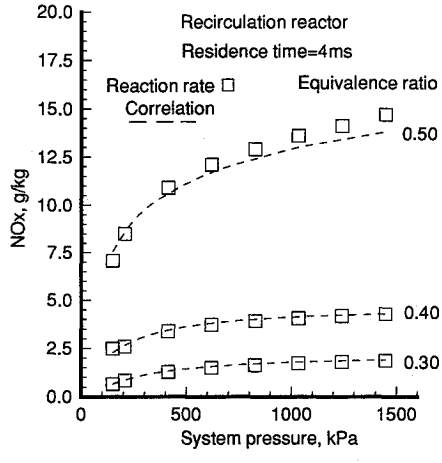

Fig. 5 Effect of pressure on NOx formation.

Figure 4 illustrates the variation of NOx with the residence time at a number of equivalence ratio levels as given by the reaction rate scheme. Also shown in the figure are the corresponding NOx values calculated by the developed approach. It is seen that the variable rates of increase of NOx with time at different equivalent ratios are well-predicted by Eq. (17). The effect of the system pressure on the formation of NOx in the primary zone reactors, as determined by both the reaction rate model and the developed correlations, is illustrated in Fig. 5. The main conclusion drawn from this figure is that the influence of the pressure on NOx increases as the equivalence ratio is increased. This is in contrast to the fixed dependency on pressure in most of the NOx correlations reported in the literature. Once again, the figure shows that the present approach closely simulates the detailed reaction rate calculation of NOx.

A similar approach is followed to calculate the NOx formed in the pilot reactor. The effect of the liquid fuel evaporation on the NOx concentration is accounted for through the reaction temperature calculation using Eq. (16), and by few modifications to the correlations developed for the primary zone reactors. For instance, the dependency of NOx on the equivalent ratio given by Eq. (18) is replaced here by

$$N_\phi = 2.8 - 8.4\phi_p + 7.4\phi_p^2 + 2.3\phi_p^3 \quad (30)$$

where ϕ_p is the equivalent ratio in pilot reactor, and the parameter an_ϕ used to calculate the residence time exponent an is given by

$$an_\phi = 0.1\phi_p^{-1.1} \exp(2.73\phi_p^{1.6}) \quad (31)$$

A value of 1.176 is used for the factor f of Eq. (23).

The formation of NOx in the main reactor, shown in Fig. 1, depends to a certain degree on the upstream reaction mechanism in the primary zone. For instance, a longer residence time in the recirculation reactor helps to bring the reaction to near completion, thus bringing up the reaction temperature in the main reactor Tm closer to the equilibrium level. The proposed NOx expression for the main zone accounts for the upstream reaction time τ_r as follows:

$$\mathrm{NOx} = Ntm \cdot N_{\phi m} \cdot [(P_3/207)^{c2} \cdot \exp[d2(P_3^{-0.2} - 0.344)](\tau_m/2)^{an} \quad (32)$$

where

$$N_m = 0.285E - 4T_m^{2.1} \exp(-1.15E5T_m^{-1.3}) \quad (33)$$

$$N_{\phi m} = (4.0 - 21.3\phi_m + 32.7\phi_m^2 + 24.4\phi_m^3 - 46\phi_m^4)(\tau_r/2)^{nm} \quad (34)$$

The exponent nm is calculated from

$$nm = -(6.7 - 140.8\phi_m + 1167.5\phi_m^2 - 4511\phi_m^3 + 8191.7\phi_m^4 - 5644.8\phi_m^5) \quad (35)$$

The parameters appearing in Eq. (32) are defined as follows:

$$c2 = 2.48 - 8.26\phi_m \quad (36)$$

$$d2 = 31.74 - 89\phi_m \quad (37)$$

The exponent an is calculated from Eq. (23) with a value of factor f of 1 and modified an_ϕ as follows:

$$an_\phi = 0.00011\phi_m^{-3.85} \exp(16\phi_m^{1.35}) \quad (38)$$

To evaluate the accuracy of the NOx correlations developed for the main reactor in simulating the detailed reaction scheme, the NOx concentration as given by both the reaction rate calculation and the correlations are plotted in Fig. 6. The results shown in this figure indicate that the additional NOx formed in the main reactor is rather limited, except for higher equivalence ratio conditions. It is also seen in the figure that the developed correlations well-predict the trends of NOx formation obtained using the chemical kinetic scheme. The NOx formed in the main reactor under a wide range of system pressure is calculated using the reaction scheme and is plotted in Fig. 7. It is obvious that the variation of NOx with pressure is not significant over most of the pressure and equivalence ratio ranges employed in this study. The results of the NOx formation as given by the developed correlations are also

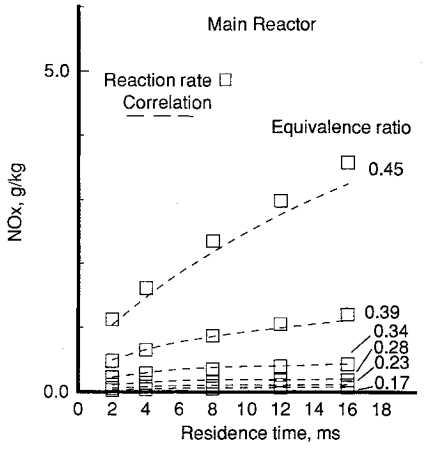

Fig. 6 NOx formation in the main reactor.

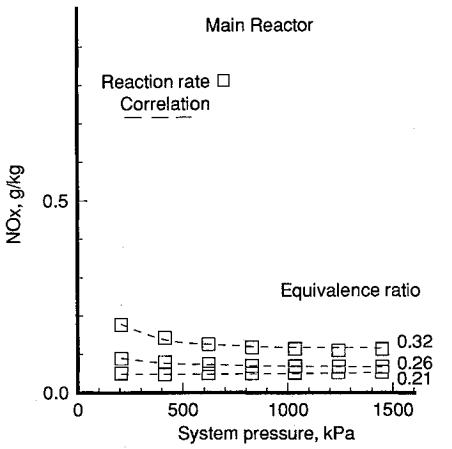

Fig. 7 Variation of NOx with pressure in main reactor.

shown in the figure to illustrate their capabilities to simulate the reaction rate mechanism.

The correlation to calculate the dilution zone contribution to the total formation of NOx was also based on the results provided by a detailed reaction rate scheme for an operating range that is typical of lean combustor concepts. The proposed equation is as follows:

$$\mathrm{NOx} = 0.0015(T_d/1329.6)^{14.4}\tau_d^{0.44} \quad (39)$$

T_d and τ_d are reaction temperature and residence time, respectively, in the dilution reactor.

The total NOx produced in the prevaporized/premix lean combustor is calculated by adding the NOx formed in all the reactors of the flow model, after adjusting the values according to the fraction of the total fuel flow in each reactor. By these means, the relative contributions of various combustor zones could be easily evaluated. In the next section, the proposed NOx model is applied to predict the NOx formation in the AGT 100 combustor. The details of the combustor configuration and the model validation effort are described in that section.

IV. NOx Model Validation

To evaluate the capability of the developed NOx model to predict the trends of formation of NOx in practical lean combustors, a data set obtained for the combustor of the automotive gas turbine engine (AGT 100) was used for model validation. In the next subsection, the combustor geometry is described, followed by the analysis of the combustor flowfield that provides some insight into the flow characteristics of various combustor regions. The application of the NOx model to the AGT 100 combustor is presented later in this section.

A. Combustor Geometry

The main features of the AGT 100 combustor are shown in Fig. 8. The combustor consists of a prechamber, in which the fuel is vaporized and mixed with air, pilot and igniter chamber, and the main cylindrical chamber of 127 mm diam. The prechamber contains a centerbody that accommodates a starter fuel nozzle located on the combustor centerline and main fuel injector. The fuel is vaporized within the prechamber because of the high temperature of the prechamber walls and the inlet air. Air is admitted into the prechamber through both axial and radial swirlers.

Engine lightoff is initiated in a pilot chamber located on the side of the main combustor chamber. The pilot chamber accommodates a fuel nozzle surrounded by a small air swirler and igniter. The pilot nozzle acts as initial ignition source, and as a sustainer source at low burner inlet temperature and/or at conditions outside the lean blowout limits.

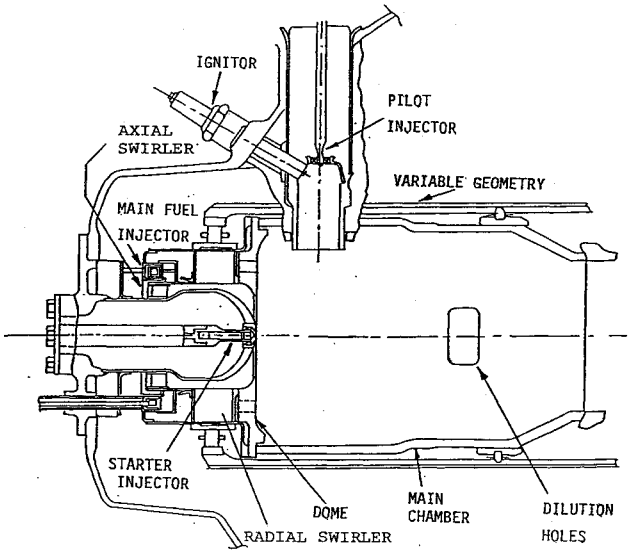

Fig. 8 Lean premix/prevaporized combustor.

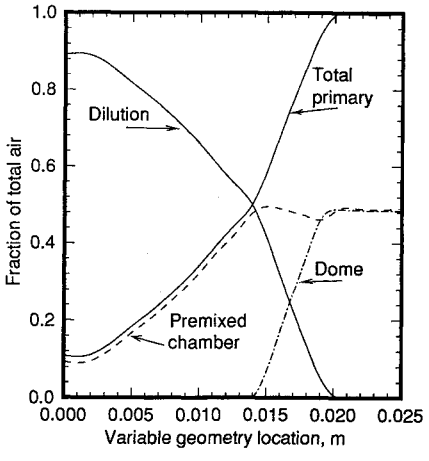

Fig. 9 Combustor inlet air distribution.

The premixed/prevaporized fuel/air mixture flows into the main chamber through a 46.6-mm-diam opening in the center of the dome. At higher power settings, additional air is admitted into the main chamber through eight holes drilled in the dome disk in such a way as to impart a swirl to the flowing air. Dilution air is admitted through four rectangular holes. A variable geometry feature is employed in the design to control the stoichiometry in the primary combustion zone by means of sliding bands. They control the available area for air to flow through the dilution holes and the radial swirler of the prechamber. At or near maximum power, the continuous motion of the variable geometry uncovers additional inlet ports that admit air into the main chamber through the dome holes.

The calculation of the available open area for airflow through each entry hole of the combustor was performed at each variable geometry location to enable estimating the airflow rate to various combustion zones. The results of the calculations are plotted in Fig. 9, as fractions of total air vs the sliding bands movement. At starting and low power modes, most of the air is admitted through the dilution holes. As the fuel flow rate is increased above idle, the variable geometry must be moved to introduce more air into the fuel preparation zone by uncovering the radial swirler and increasing the blockage of the dilution holes. This figure is used to evaluate the air distribution to various combustor zones needed in the validation effort of the NOx model.

The combustor instrumentation included four radial rakes, each having four sampling openings located in equal area zones across the exit flow path. The emissions were measured over ranges of inlet temperatures of 1000–1233 K, inlet pressures of 133–414 kPa, fuel/air ratios of 0.0031–0.01, and airflow rates of 0.08–0.27 kg/s.

B. Three-Dimensional Combustor Flowfield Analysis

Multidimensional calculations provide detailed information on the combustor internal flowfield, such as fuel distribution in the liner, gas temperatures, and recirculation zones. The analysis can give insight into potential regions of excessive formation of NOx and/or incomplete combustion. A finite difference code that solves the Navier-Stokes equations for a reacting flowfield was used in the present investigation to guide the selection of the details of the NOx flow model. The program simulates turbulence by the two-equation k-ε model,[20,21] and combustion following vaporization is determined by a four-step chemical reaction model based on Arrhenius and eddy breakup concepts.[22]

A 90-deg sector of the AGT 100 combustor was divided into 39 × 28 × 29 finite difference nodes along axial, radial, and circumferential directions, respectively. Examples of the three-dimensional results are given in computer-drawn plots of selected longitudinal sections of the combustor sector. A number of combustor settings were selected for the three-dimensional analysis to investigate the variation of the details of the flowfield with operating conditions. Figure 10 shows the velocity vectors in a plane that passes through a dilution hole for variable geometry positions of 0.005 and 0.015 m. The angle Z defines the location of the longitudinal plane within the 90-deg sector of the modeled combustor. The figure shows that the recirculating flow pattern in the primary zone is well-defined, in particular, at the larger variable geometry setting. This recirculation region plays a significant role in stabilizing the flame in the combustor. Meanwhile, as less air becomes available for the dilution zone, the jet penetration and the effects on the flow in its vicinity are significantly reduced.

The contours of the fuel/air ratio for the two positions of the variable geometry device are illustrated in Fig. 11. Significantly higher levels of fuel/air ratio occur in the recirculation region of the first case, when less air is admitted through the combustor prechamber, than in the second case. Fuel/air ratio gradients caused by the dilution jet vary according to the variable geometry setting used in the test.

The corresponding gas temperature contours are given in Fig. 12 for the two combustor settings. A region of high gas temperature is observed in the recirculation zone for the variable geometry position of 0.005 m. This region is responsible

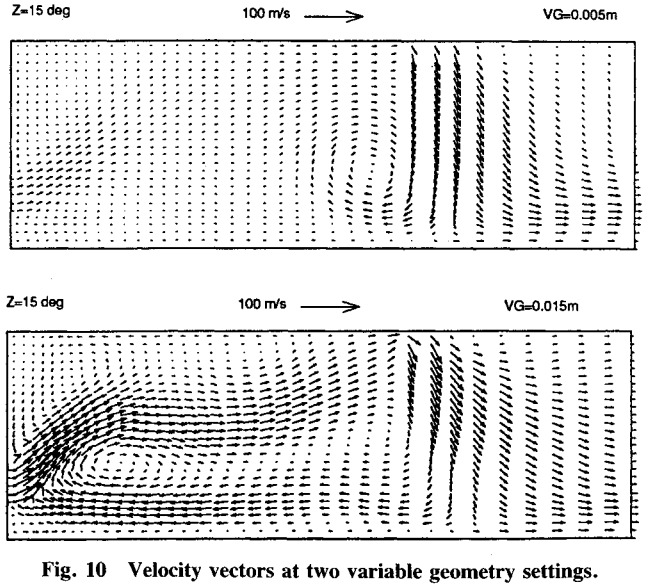

Fig. 10 Velocity vectors at two variable geometry settings.

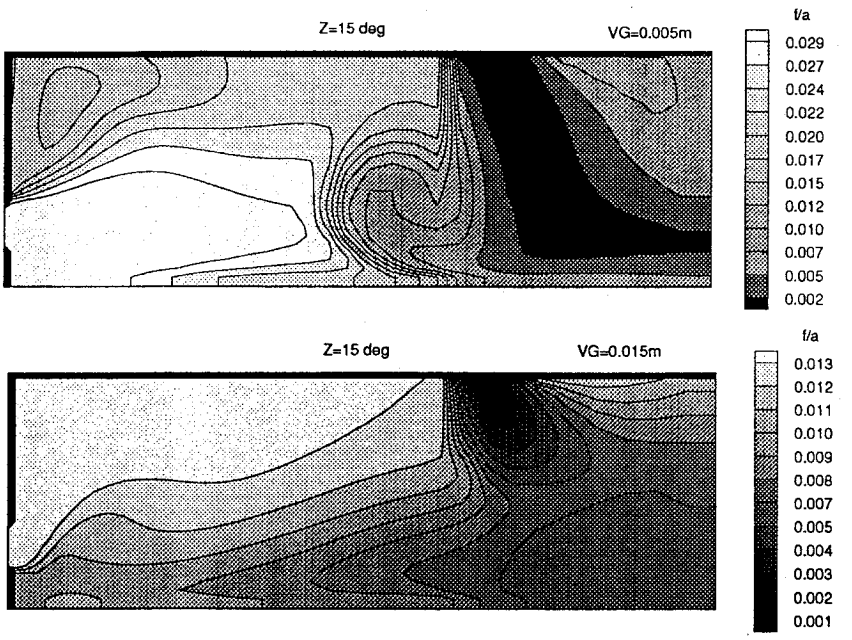

Fig. 11 Fuel/air ratio contours in combustor.

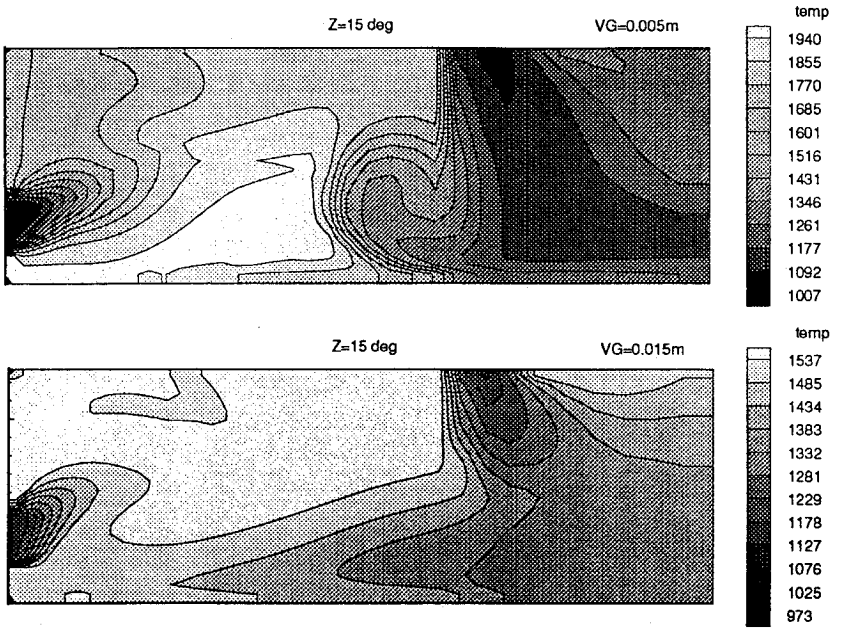

Fig. 12 Gas temperature contours for two operating modes.

for most of the high level of NOx of 4.5 g/kg measured under this particular setting. Relatively high-temperature regions also extend to the near-wall and downstream zones of the combustor. Less favorable conditions for NOx formation occur in the second setting. In fact, considering that the pilot operated in the test at this setting, the measured NOx was 1.45 g/kg, which was almost one-third the value measured in the first case.

It is seen that the utilization of the three-dimensional analysis provides useful information in regard to the flowfield characteristics of the combustor. Details of recirculation region and dilution jet mixing can assist in defining various combustor regions required in the modeling of emissions. It has been shown in an earlier effort that the prediction capability of these models is significantly improved by combining the models with three-dimensional analytical tools.[23] By this means, modifications to the combustor design for reduced emission formation could be more easily facilitated.

C. Combustor NOx Calculations

The data set of the AGT 100 combustor was used to evaluate the NOx calculation concept presented in the previous section. To determine the equivalence ratio and residence time in the reactors of the combustor flow model shown in Fig. 1, the flow split and volume of each reactor needed to be defined. The reaction rate mechanism was used to calculate the residence time of the recirculation reactor using the lean blowout characteristics of the combustor. The fuel/air ratio at lean blowout varied over a wide range, depending on operating conditions and variable geometry position. A value of 0.0035 was measured at a 1033 K inlet temperature, and a variable geometry position of 0.0076 m.

Defining a parameter $F1$ that describes the fraction of the air/fuel vapor mixture entering the recirculation reactor, and taking into consideration the air flowing through the dome holes, enable calculating the geometry of the primary zone reactors. Based on information given by the three-dimensional

Table 1 Predictions of the NOx model

Variable geom. position, m	NOx calculation, g/kg					NOx measurement
	Recirculation	Near wall	Pilot	Main	Total	
0.0051	3.66	0.41	0.00	0.62	4.68	4.50
0.0076	0.56	0.06	1.92	0.14	2.68	2.39
0.0076	0.58	0.06	0.00	0.07	0.71	0.87
0.0102	1.24	0.14	0.66	0.20	2.24	2.32
0.0102	0.33	0.02	0.00	0.04	0.39	0.60
0.0114	0.61	0.05	2.23	0.11	3.00	2.92
0.0114	0.55	0.05	0.00	0.08	0.69	0.64
0.0127	0.56	0.05	1.98	0.09	2.68	2.75
0.0127	0.34	0.01	0.00	0.03	0.37	0.45
0.0152	0.50	0.00	0.85	0.07	1.42	1.45
0.0178	0.42	0.00	0.79	0.04	1.24	1.16
0.0203	0.37	0.00	0.64	0.03	1.05	0.99

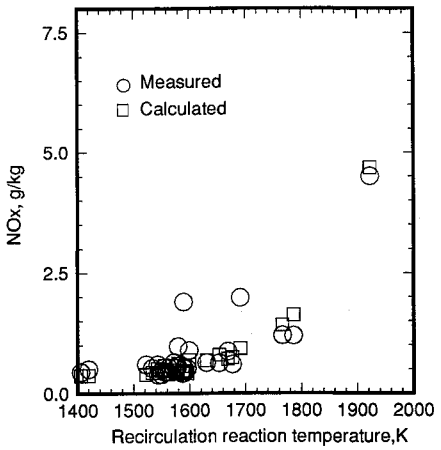

Fig. 13 NOx model predictions for AGT 100 combustor.

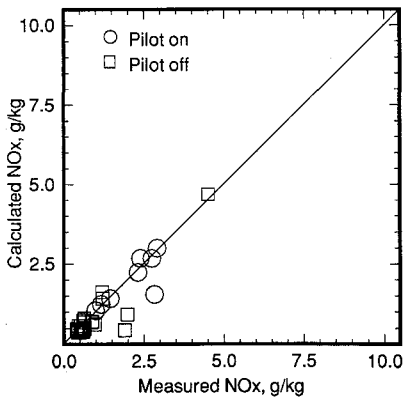

Fig. 14 Overall comparison between calculated and measured NO.

analysis, it was estimated that 10% of the total prechamber flow reaches the near-wall reactor. Although the selection of the parameter $F1$ may have an insignificant effect on overall NOx formation, it will surely influence the levels of CO produced in the near-wall region. The dimensions of the main and the dilution reactors are taken from the combustor configuration.

The developed model was then used to calculate the NOx formation under various combustor operating conditions. The results are plotted against the calculated reaction temperature of the recirculation reactor, together with the measured NOx values, in Fig. 13. The figure clearly shows the trend of the increase in NOx formation with the rise in the reaction temperature. Very satisfactory agreement between the measurements and the calculations is achieved for almost all the data points. The experimental data shown in this figure were obtained when the combustor operated with no pilot.

The results obtained when both the main and pilot fuel injectors were employed in the test have shown a significant increase in NOx over the values measured under similar conditions with no pilot in operation. The results also indicated that increasing combustor pressure drop and/or reducing the pilot fuel flow resulted in more formation of NOx. This is attributed to the enhanced spray quality and evaporation rate achieved in the pilot chamber under these conditions that cause the reaction to occur at a higher temperature over a longer period of time.

The effects of evaporation and mixing in the pilot reactor are accounted for by the following equation:

$$\mathrm{NOx} = \mathrm{NOo}[1.294(\Delta P_3/P_3)^{0.5}/\phi_p^{3.0}] \qquad (40)$$

where NOo is the value of pilot NOx as calculated by the approach given in the previous section, $\Delta P_3/P_3$ is combustor pressure drop, and ϕ_p is the pilot equivalence ratio. The constant appearing in Eq. (40) is a result of using the ratios of the parameters within the brackets with respect to reference values. Figure 14 shows a comparison between the calculated values of NOx, with and without pilot operation, and the corresponding measured data. The figure indicates that the present approach gives satisfactory agreement with the measurements over the whole range of operation.

Table 1 includes the results of the calculations for a number of operating conditions to illustrate the relative contributions of various combustion zones to the total NOx formed in the combustor. The experimental measurements and relevant operating parameters are also given in the table.

The obvious advantage offered by the developed NOx model is the capability to provide insight into the process of NOx formation within various regions of the lean prevaporized/premixed combustor. Thus, the effort to reduce the NOx from this combustor concept could be more efficiently performed. The fact that the NOx model was based on a detailed chemical reaction scheme, makes the NOx results more realistic, with significantly less computation effort. The next phase of activity will address the improvement of the hybrid analytical/empirical approach described in a previous section by utilizing the developed NOx model to replace the currently used empirical expressions. A similar approach has been successfully developed in early effort for diffusion flame combustors.[23]

V. Summary and Conclusions

The present investigation involves the development of a model to calculate the NOx formation in the lean prevaporized/premixed gas turbine combustor. In this model, the combustor primary zone is simulated by a number of stirred reactors that represent the primary zone recirculation zone, the near-wall region, and the pilot chamber. The outcome of these reactors mix together to form a main plug reactor where the balance of fuel is oxidized. Air is admitted downstream of the main reactor to form a plug reactor that simulates the

dilution zone. A reaction mechanism that combined a global rate equation for hydrocarbons breakdown with finite rate equations for CO and H_2 combustion and NO formation was used to provide the trends of formation of NOx in various combustor zones.

Based on these results, expressions to calculate the reaction temperature and NOx concentration in terms of operating conditions and equilibrium temperature were developed. The simulation of the reaction mechanism by the developed expressions is supplemented by the inclusion of the effects of fuel evaporation and mixing in the pilot chamber of the combustor. The agreement between the NOx calculated using the proposed model and results provided by the reaction rate scheme is very satisfactory. Moreover, the effects of such parameters as pressure, residence time, and combustor air distribution are better understood in light of the results offered by the proposed NOx model.

The model validation involved the calculation of the NOx formed in the variable geometry lean combustor of the AGT 100 engine under various operating modes. In addition to enhancing the capability to provide accurate estimates of NOx, the model provides insight into the relative contributions of the primary zone and the pilot chamber to the total NOx in the combustor. For instance, the model shows that a significant amount of NOx could form in the pilot, thus partially offsetting the advantage offered by the lean prevaporization/premix combustion concept in producing ultralow levels of NOx. It is also found in this investigation that the utilization of analytical tools to evaluate the combustor flowfield characteristics provides valuable information to the modeling effort. In the next phase of activity, the developed NOx model will be combined with a three-dimensional combustor performance code to form a hybrid approach. By these means, the effects of changing the details of the combustor configuration on its performance could be readily determined.

Acknowledgment

The authors would like to thank G. Miles of Allison Gas Turbine Division for his effort in preparing the chemical kinetic scheme used in the present investigation.

References

[1]Novick, A. S., and Troth, D. L., "Low NOx Heavy Fuel Combustor Concept Program," NASA CR-165367, DOE-NASA-0148-1, Oct. 1981.

[2]Rizk, N. K., and Mongia, H. C., "Ultra-Low NOx Rich-Lean Combustion," American Society of Mechanical Engineers Paper 90-GT-87, June 1990.

[3]Anderson, D. A., "Ultra-Lean Combustion at High Inlet Temperatures," American Society of Mechanical Engineers Paper 81-GT-44, March 1981.

[4]Smith, K. O., Angello, L. C., and Kurzynske, F. R., "Design and Testing of an Ultra-Low NOx Gas Turbine Combustor," American Society of Mechanical Engineers Paper 86-GT-263, June 1986.

[5]Duerr, R. A., and Lyons, V. J., "Effect of Flameholder Pressure Drop on Emissions and Performance of Premixed Prevaporized Combustors," NASA TP 2131, April 1983.

[6]Ross, P. T., Williams, J. R., and Anderson, D. A., "Combustor Development for Automotive Gas Turbines," *Journal of Energy*, Vol. 7, No. 5, 1983, pp. 429–435.

[7]Sasaki, M., Kumakura, H., and Suzuki, D., "Low NOx Combustor for Automotive Ceramic Gas Turbine—Conceptual Design," American Society of Mechanical Engineers Paper 91-GT-369, June 1991.

[8]Lefebvre, A. H., "Fuel Effects on Gas Turbine Combustion—Liner Temperature, Pattern Factor, and Pollutant Emissions," *Journal of Aircraft*, Vol. 21, No. 11, 1986, pp. 887–898.

[9]Mellor, A. M., "Gas Turbine Engine Pollution," *Progress in Energy and Combustion Science*, Vol. 1, Pergamon, Oxford, England, UK, 1976, pp. 111–133.

[10]Rizk, N. K., and Mongia, H. C., "Lean Low NOx Combustion Concept Evaluation," *23rd Symposium (International) on Combustion*, The Combustion Inst., Pittsburgh, PA, 1990, pp. 1063–1070.

[11]Mongia, H. C., Reynolds, R. S., and Srinivasan, R., "Multidimensional Gas Turbine Combustion Modeling: Applications and Limitations," *AIAA Journal*, Vol. 24, No. 6, 1986, pp. 890–904.

[12]Rizk, N. K., and Mongia, H. C., "Three-Dimensional Combustor Performance Validation with High Density Fuels," *Journal of Propulsion and Power*, Vol. 6, No. 5, 1990, pp. 660–667.

[13]Rizk, N. K., and Mongia, H. C., "Three-Dimensional Analysis of Gas Turbine Combustors," *Journal of Propulsion and Power*, Vol. 7, No. 3, 1991, pp. 445–451.

[14]Rizk, N. K., and Mongia, H. C., "Low NOx Rich-Lean Combustion Concept Application," AIAA Paper 91-1962, June 1991.

[15]Rizk, N. K., and Mongia, H. C., "Semianalytical Correlations for NOx, CO, and UHC Emissions," *Journal of Engineering for Gas Turbines and Power, Transactions of the American Society of Mechanical Engineers*, Vol. 115, 1993, pp. 612–619.

[16]Buchheim, R., "Influences on Exhaust Emissions from Automotive Gas Turbines," American Society of Mechanical Engineers Paper 78-GT-85, April 1978.

[17]Glassman, I., *Combustion*, Academic Press, New York, 1977.

[18]Hammond, D. C., Jr., and Mellor, A. M., "Analytical Predictions of Emissions from and Within an Allison J-33 Combustor," *Combustion Science Technology*, Vol. 6, 1973, pp. 279–286.

[19]Fletcher, R. S., and Heywood, J. B., "A Model for Nitric Oxide Emissions from Aircraft Gas Turbine Engines," AIAA Paper 71-123, 1971.

[20]Patankar, S. V., *Numerical Heat Transfer and Fluid Flows*, Hemisphere, Washington, DC, 1980.

[21]Launder, B. E., and Spalding, D. B., "The Numerical Computation of Turbulent Flow," *Computer Methods in Applied Mechanics and Engineering*, Vol. 3, 1976, pp. 269–289.

[22]Hautman, D. J., Dryer, F. L., Schug, K. P., and Glassman, I., "A Multiple-Step Overall Kinetic Mechanism for the Oxidation of Hydrocarbons," *Combustion Science and Technology*, Vol. 25, 1981, pp. 219–235.

[23]Rizk, N. K., and Mongia, H. C., "Three-Dimensional Gas Turbine Combustor Emissions Modeling," *Journal of Engineering for Gas Turbines and Power, Transactions of the American Society of Mechanical Engineers*, Vol. 115, 1993, pp. 603–611.